

Bewick, R. and Sanchez, J.P. and McInnes, C.R. (2010) An L1 positioned dust cloud as an effective method of space-based geoengineering. In: International Astronautical Congress, IAC 2010, 27 September - 1 October 2010, Prague, Czech Republic.

<http://strathprints.strath.ac.uk/27439/>

Strathprints is designed to allow users to access the research output of the University of Strathclyde. Copyright © and Moral Rights for the papers on this site are retained by the individual authors and/or other copyright owners. You may not engage in further distribution of the material for any profitmaking activities or any commercial gain. You may freely distribute both the url (<http://strathprints.strath.ac.uk>) and the content of this paper for research or study, educational, or not-for-profit purposes without prior permission or charge. You may freely distribute the url (<http://strathprints.strath.ac.uk>) of the Strathprints website.

Any correspondence concerning this service should be sent to The Strathprints Administrator: [eprints@cis.strath.ac.uk](mailto:eprints@cis.strath.ac.uk)

IAC-10-D1.1.7

## AN L<sub>1</sub> POSITIONED DUST CLOUD AS AN EFFECTIVE METHOD OF SPACE-BASED GEOENGINEERING

**Russell Bewick**

Advanced Space Concepts Laboratory, University of Strathclyde,  
Glasgow, UK, russell.bewick@strath.ac.uk

J.P. Sanchez<sup>\*</sup>, C. McInnes<sup>†</sup>

### ABSTRACT

In this paper a method of geoengineering is proposed involving clouds of dust placed in the vicinity of the L<sub>1</sub> point as an alternative to the use of thin film reflectors. The aim of this scheme is to reduce the manufacturing requirement for space-based geoengineering. It has been concluded that the mass requirement for a cloud placed at the classical L<sub>1</sub> point, to create an average solar insolation reduction of 1.7%, is  $2.93 \times 10^9$  kg yr<sup>-1</sup> whilst a cloud placed at a displaced equilibrium point created by the inclusion of the effect of solar radiation pressure is  $8.87 \times 10^8$  kg yr<sup>-1</sup>. These mass ejection rates are considerably less than the mass required in other unprocessed dust cloud methods proposed and, for a geoengineering period of 10 years, they are comparable to thin film reflector geoengineering requirements. It is envisaged that the required mass of dust can be extracted from captured near Earth asteroids, whilst stabilised in the required position using the impulse provided by solar collectors or mass drivers used to eject material from the asteroid surface.

### I. INTRODUCTION

The current consensus within the scientific community is that climate change is not only happening but is almost unavoidable. Projections made using climate models over recent years have suggested that the mean global temperature is likely to increase by 1.1-6.4°C by the end of this century [1]. With the continuing industrialisation of the developing world and the lack of an agreed international protocol on tackling of greenhouse gas emissions, this temperature increase seems unstoppable. While the focus of international efforts should remain with the attempts to prevent climate change by the reduction of greenhouse gas emissions, it is prudent to investigate methods to mitigate its effects. This can be achieved by the deliberate manipulation of the Earth's climate, commonly referred to as climate engineering or geoengineering.

Several proposals for possible geoengineering methods have been made and these can generally be placed in two categories; solar radiation management and carbon sequestration [2]. Solar radiation management focuses on the reduction of the amount of sunlight being absorbed by the Earth's atmosphere by either increasing the Earth's albedo, e.g. through using more reflective roofing materials, or by reducing the level of sunlight reaching the surface, e.g. by placing aerosol particles into the stratosphere to reflect sunlight. Alternatively carbon capture techniques aim to deal with the fundamental cause of global warming by either direct or indirect methods. Direct methods include schemes such as capturing CO<sub>2</sub> from the air and placing it into storage, whilst an example of an indirect method is the fertilisation of the ocean to stimulate increased algal growth with these algae then leading to increased CO<sub>2</sub> uptake.

A report into geoengineering conducted by the Royal Society in 2009 [2] examines the feasibility of all types of schemes based on the criteria of effectiveness, affordability, timeliness and safety. In general the report appears to show that there is no perfect solution with the schemes that appear most effective suffering in other criteria such as affordability. One of the most effective solutions

---

<sup>\*</sup> ASCL, University of Strathclyde, Glasgow, UK, jpau.sanchez@strath.ac.uk

<sup>†</sup> ASCL, University of Strathclyde, Glasgow, UK, colin.mcinnis@strath.ac.uk

suggested is the use of space-based solar reflectors to reduce incident solar insolation. Whilst this technique does not appear to be affordable or timely, it does have a key advantage over other schemes; the Earth itself does not need to be physically changed. This is a significant advantage when compared to schemes which involve ejecting large quantities of sulphur particles into the stratosphere or iron into the ocean, where the precise effect of the changed chemistry cannot be fully known.

It has been estimated that in order to offset the effects of global warming caused by a doubling of the  $CO_2$  concentration (compared to pre-industrial levels and corresponding to an increase in global temperature of approximately  $2^\circ C$ ) solar insolation must be reduced by 1.7% [3]. Similarly for a quadrupling of  $CO_2$  the required insolation change is 3.6% [4].

There have been several different proposals to date regarding the reduction of solar insolation using space-based methods the key characteristics of which can be seen in Table 1. The methods either utilise a cloud of dust [5-6] or solid reflectors or refractors [5, 7-10] to reduce the level of solar insolation. Typically the methods that require the least mass are those that use solid reflectors/refractors whilst the mass for dust cloud methods are orders of magnitude higher. This is mostly due to the increased level of control that can be placed upon the solid reflectors, hence they can be stationed in optimum positions. Dust clouds cannot be controlled and can only be placed with suitable initial conditions, with subsequent replenishment necessary due to the orbital decay or perturbation of the particle orbits. Conflicting with this, though, is the consideration of the engineering complexity of the system. Whilst dust clouds are a relatively crude method, the material can be readily produced with little processing required, whereas solid reflectors must be manufactured on Earth and then launched into position or manufactured in-situ. Clearly taking this into account, the low rating for affordability and timeliness indicated in the Royal Society report can be understood.

The method proposed by Pearson [5] to place a ring of dust or reflecting satellites in Earth orbit, though comparatively low in mass, clearly has possible side effects including an increased danger to Earth orbiting satellites. Additionally the ring will have the effect of increasing reflected light onto the night side of the Earth under certain conditions. For these reasons this method is not seen as the most optimal space-based geoengineering solution.

An additional factor that affects the relative mass of the different methods is the amount of time that the reflectors spend along the Sun-Earth line. For example the method proposed by Struck [6] to place

clouds of dust at the  $L_4/L_5$  Lagrange libration points of the Earth-Moon system has a clear benefit as these points are stable. However, as these points effectively orbit around the Earth they are only occasionally in a position to reduce solar insolation. Furthermore, the movement of the clouds will create a flickering effect. On most occasions there will be no change in insolation whilst at those times when the cloud is present the insolation change required will be much greater than the net 1.7% reduction.

Ultimately none of these concepts are ideal for geoengineering, though should the technology become available and the necessity to act quickly on climate change become apparent they could still perhaps be implemented. The aim of this paper is to propose a simplified space-based geoengineering method with the aim of improving the timeliness and affordability of the dust-based systems by placing clouds of dust at the Sun-Earth  $L_1$  point. An example of this concept can be seen in Fig. 1.

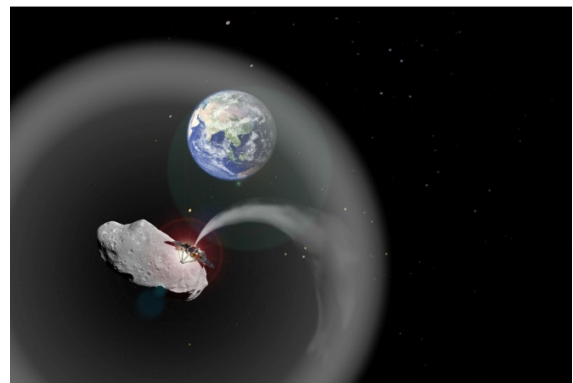


Fig. 1: Impression of an  $L_1$  positioned dust cloud for space-based geoengineering.

The feasibility of this method shall be explored by first investigating the dynamics of the  $L_1$  point. It is well known that the  $L_1$  point is unstable, but it is none-the-less an equilibrium point where particles could remain for a significant period of time given appropriate initial conditions. Therefore, this paper will use an analysis of the stability properties to make an estimate of the average lifetime of a dust cloud with different cloud radii, different sizes of dust grains and their initial conditions. The optimum initial conditions of the cloud can then be found to maximise the net insolation reduction.

Subsequently, the ability of the cloud to reduce solar insolation will be investigated. This will be achieved by means of a solar radiation model (SRM). The model will initially be used to determine the characteristics of the cloud that most efficiently creates the required reduction in solar insolation. The variables in this case will be the cloud size as well as the grain radius and number density. Subsequently the

SRM will be used to analyse the ability of the optimum dust cloud to reduce solar insolation.

Position	Type	Mass [kg]	Reference
Earth Orbit	Dust	$2.3 \times 10^{12}$	[5]
Earth Orbit	Solar Reflector	$5.0 \times 10^9$	[5]
Earth-Moon	Dust	$2.1 \times 10^{14}$	[6]
L <sub>4</sub> /L <sub>5</sub>			
Sun-Earth	Solar Reflector	$2.6 \times 10^{11}$	[7]
L <sub>1</sub>			
Sun-Earth	Solar Refractor	$2.0 \times 10^{10}$	[10]
L <sub>1</sub>			

Table 1: The key characteristics of proposed space-based geoengineering schemes to reduce solar insolation by 1.7%.

## II. DUST DYNAMICS

The following section will detail the dynamics of a dust cloud in the vicinity of the interior Lagrange point in the Sun-Earth three body problem.

### II.1 Three-Body Problem

The cloud shall be assumed to be moving in a system where only the gravitational forces due to the Sun and the Earth are significant. Hence, the circular restricted three-body problem (CR3BP) shall be used to describe the motion of the dust particles in the cloud. The dimensionless equations of motion in a rotating reference frame are given by;

$$\begin{aligned} \ddot{x} - 2\dot{y} &= -\frac{\partial U}{\partial x} \\ \ddot{y} + 2\dot{x} &= -\frac{\partial U}{\partial y} \\ \ddot{z} &= -\frac{\partial U}{\partial z} \end{aligned} \quad (1)$$

where the non-dimensional potential function,  $U$ , is;

$$U(x, y, z) = \frac{1}{2}(x^2 + y^2) + \frac{1-\mu}{\rho_1(x, y, z)} + \frac{\mu}{\rho_2(x, y, z)} \quad (2)$$

Here the mass ratio of the secondary to total system mass is  $\mu$  and the parameters  $\rho_{1,2}$  are the distances of the particle to each of the primary and secondary

masses, (3), as shown in Fig. 2. In dimensionless coordinates the Sun and Earth are positioned at  $M_1 (-\mu, 0, 0)$  and  $M_2 (1-\mu, 0, 0)$  respectively. Hence;

$$\begin{aligned} \rho_1 &= \sqrt{(x+\mu)^2 + y^2 + z^2} \\ \rho_2 &= \sqrt{(x+\mu+1)^2 + y^2 + z^2} \end{aligned} \quad (3)$$

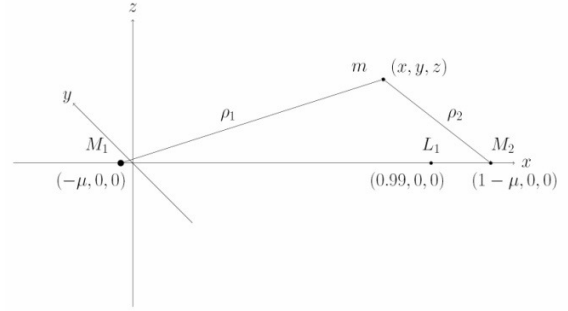


Fig. 2: Geometry of the circular restricted three-body problem with Sun  $M_1$ , Earth  $M_2$  and dust grain  $m$ .

The equilibrium, or libration points, are located where the combined gravitational force of the two primary bodies on a particle is equal to the centripetal force required for it to orbit in a fixed position relative to the two primary bodies. These positions can be found by finding the stationary points of the potential function (1). In particular, the equilibrium points required for this geoengineering method must lie along the Sun-Earth line and must therefore lie along the  $x$  axis hence  $y=z=0$ . Using (1), the position of the L<sub>1</sub> point can be found by numerically finding the roots of (4);

$$x - \frac{1-\mu}{(x+\mu)^2} + \frac{\mu}{(x-1+\mu)^2} = 0 \quad (4)$$

For the Sun-Earth system the L<sub>1</sub> point is located approximately at (0.99,0,0), or  $1.5 \times 10^6$  km from the Earth.

### II.2 Effect of Solar Radiation Pressure

An additional factor that must be considered is the effect of solar radiation pressure (SRP). This is created by the transfer of momentum from solar photons to bodies with which the photons interact. Generally the effect of SRP is relatively small due to the large mass of conventional satellites. However, for dust particles this is not the case. Here the surface area to mass ratio is large and therefore a significant momentum transfer will take place between solar photons and the dust particles. The effect of SRP can be quantified using the 'lightness' parameter,  $\beta$ ,

which is the ratio of the force due to SRP and solar gravity. This can be calculated using [11];

$$F_{rad} = \frac{L_{\odot} \sigma_{gr} Q}{4\pi c r_{\odot}^2} \quad (5)$$

where  $L_{\odot}$  is the solar luminosity,  $\sigma_{gr}$  is the grain cross-sectional area,  $c$  is the speed of light,  $r_{\odot}$  is the distance to the Sun and  $Q$  is the radiation pressure coefficient. As  $\beta$  is the ratio of the two forces it now follows that the  $\beta$ -value can be determined as;

$$\beta = \left| \frac{F_{rad}}{F_g} \right| \approx 570 \frac{Q}{\rho R_{gr}} \quad (6)$$

where  $\rho$  is the grain density and  $R_{gr}$  is the radius of the grain. The parameter  $Q$  determines the coupling effect of SRP and is dependent upon the material which the dust is comprised of. For example, a completely transparent material will have a value of  $Q=0$  whilst for a completely absorbing grain  $Q=1$  and for a completely reflecting grain  $Q=2$ .

For relatively large radius particles,  $R_{gr} > 1\mu\text{m}$ , the value of  $Q$  varies little but as the size decreases the interaction between the solar photons and the dust grains becomes more complex. Wilck and Mann [12] determine the  $\beta$ -value for a range of particle radii using Mie theory using different composition models. The results for a typical asteroidal dust grain can be seen in Fig. 3. This shows that the  $\beta$ -value peaks at a value of approximately 0.9 at a radius of  $0.2\mu\text{m}$  before decreasing to 0.1 for a radius of  $0.01\mu\text{m}$ .

Due to the nature of the SRP, the effect is to reduce the effective gravity of the Sun and hence the magnitude of this force is now;

$$F_{g,eff} = (1 - \beta) \frac{GM_{\odot} m_{gr}}{r_{\odot}^2} \quad (7)$$

In the case of the mass parameter,  $\mu$ , for the 3 body problem is now;

$$\mu = \frac{M_2}{M_2 + (1 - \beta)M_1} \quad (8)$$

Due to the increase in the value of  $\mu$  with increased  $\beta$  the L<sub>1</sub> equilibrium point is found to shift towards the Sun. The magnitude of this effect can be seen in Fig. 4. For particles with  $\beta > 0$  placed at the conventional L<sub>1</sub> point this displacement from the equilibrium point will lead to an increased instability timescale. Therefore, it will be best to avoid particles in the range of peak  $\beta$ , hence particles with a radius greater than  $3\mu\text{m}$  or less than  $0.03\mu\text{m}$  are preferred.

A possible beneficial effect of increased  $\beta$  is that the potential function, (2), will appear flattened at the new equilibrium point in comparison to the classical L<sub>1</sub> point. This will lead to increased stability if the dust cloud is positioned at this point, though the effect that the dust cloud has on the solar insolation reduction is likely to be reduced as a smaller solid angle is subtended when viewed from the Earth. Quantifying this effect may prove to be an interesting avenue of research.

It should be noted that it is assumed, for simplicity, that all particles within the cloud receive the same incident solar radiation. In reality this would not be the case as the attenuation of the solar photons would lead to a decreased value of  $F_{rad}$  for particles not at the Sun facing boundary of the cloud and hence the effect of SRP would reduce. The magnitude of this effect would vary depending on the size and level of insolation change required. For example a relatively small cloud may require a very large attenuation of solar radiation and hence the particles at the Earth facing boundary are likely to have a much smaller  $\beta$ -value than expected.

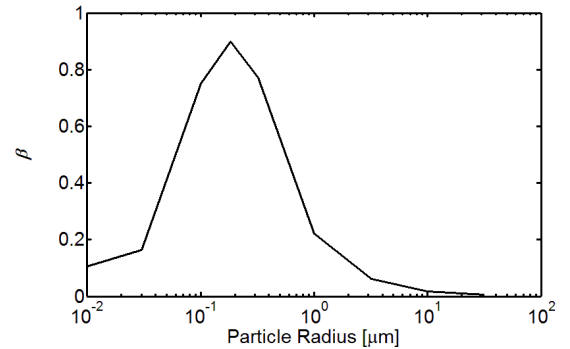


Fig. 3: Variation in  $\beta$  with particle radius for an asteroidal dust grain model as described in [12]

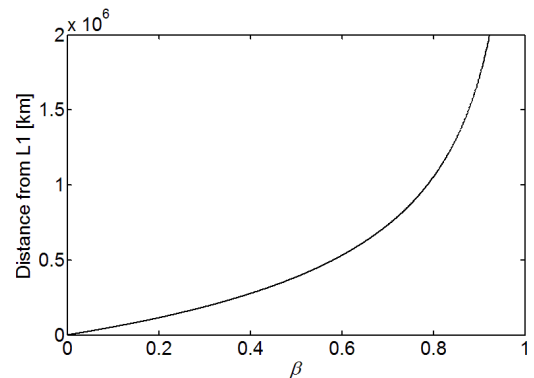


Fig. 4: Sunward distance between the conventional L<sub>1</sub> libration point in the Sun-Earth system and the equilibrium point when the effect of SRP is taken into account.

### II.III Transition Matrix

Critical to this study is the ability to predict the motion of dust particles in relation to the L<sub>1</sub> point. This is because the libration point is unstable and therefore particles will naturally drift away if there is no control strategy implemented, as is the case for a passive dust cloud. The most efficient method for determining the motion of a large group of particles is to generate a transition matrix. This can then provide the state vector,  $X(t)$ , of a particle at time  $t$  given some initial state vector (9). This state vector contains the position,  $x(t)$ , and velocity,  $v(t)$ , of a particle at time  $t$  so that;

$$X(t) = \begin{bmatrix} x(t) \\ v(t) \end{bmatrix} = \Phi(t, t_0) X(t_0) \quad (9)$$

where the transition matrix is defined by;

$$\Phi(t, t_0) = \begin{bmatrix} \frac{\partial x(t)}{\partial x(t_0)} & \frac{\partial x(t)}{\partial v(t_0)} \\ \frac{\partial v(t)}{\partial x(t_0)} & \frac{\partial v(t)}{\partial v(t_0)} \end{bmatrix} \quad (10)$$

More specifically the transition matrix includes components that allow the contribution to the final position and velocity of the initial position and velocity to be determined individually. This will also allow the initial position and velocity relative to the equilibrium point to be determined from a given point at time  $t$ . This will aid the SRM in determining the path length through a given dust cloud. For example if the initial velocity of a particle is assumed to be zero its initial position is;

$$x(t_0) = \left[ \frac{\partial x(t)}{\partial x(t_0)} \right]^{-1} x(t) \quad (11)$$

The Jacobian matrix uses the linearization of the equations of motion (1) to calculate the state vector for small time intervals. This can then be integrated to give the transition matrix (9) to propagate the state vector for a large time step from time  $t_0$  to time  $t$  [13].

An example showing the movement of a 3,000km radius cloud with a grain  $\beta$  value of 0.106 is shown in Fig. 5. It can be seen that the motion of the cloud is away from the L<sub>1</sub> point when the initial position is displaced from the equilibrium point. The original cloud becomes stretched with increasing distance from the equilibrium point as the relative dynamics of

the particles varies throughout the cloud as described by the state transition matrix (9).

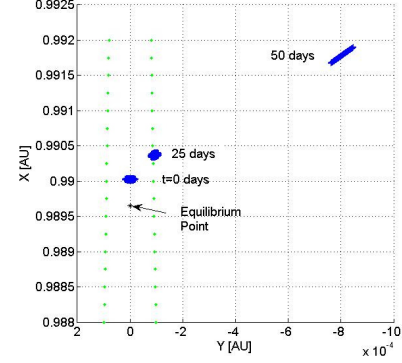


Fig. 5: Motion of a 3,000km radius spherical cloud of particles in the  $x$ - $y$  plane over a period of 50 days. The green dotted lines represent the extent of the useful zone along the Sun-Earth line.

### III. SOLAR RADIATION MODEL

The solar radiation model (SRM) is used to determine the reduction in insolation due to the presence of the dust cloud. The basic principle of the model is that the path length through the cloud can be found for a line connecting a point on the Sun's surface to a point on the Earth's surface. This path length is then used to calculate the fractional intensity through the cloud using the Beer-Lambert law for which the general case, (12), can be seen below;

$$I / I_0 = e^{-\int \alpha_{gr}(l) dl} \quad (12)$$

Here the factor  $\alpha_{gr}$  is the extinction coefficient due to the scattering and absorption of photons by a certain concentration of particles. A general approximation of this coefficient is the physical cross section,  $\sigma_{gr}$ , of the particles involved multiplied by their number density,  $\rho_n$ . The cloud is assumed to be comprised of only one size of particle and that the density is homogeneous, which simplifies the Beer-Lambert law considerably (13) so that;

$$I / I_0 = e^{-l \sigma_{gr} \rho_n} \quad (13)$$

where  $l$  is the path-length through the cloud. To calculate the intensity at the Earth's surface the initial intensity,  $I_0$ , must also be known. This can be estimated using a relation involving the solid angle subtended by a point on the Earth's surface,  $\Omega$ , the area of the point on the Sun's surface,  $A$ , and the angle of the line-of-sight to the Earth from the surface

normal of the Sun  $\theta$ , and the solar radiance,  $I_{\odot}$ , of  $2.01 \times 10^7 \text{ W m}^{-2} \text{ sr}^{-1}$  so that;

$$I_0 = I_{\odot} \Omega A \cos \theta \quad (14)$$

These principles will now be used to construct a complete solar radiation model.

### III.1 Model Structure

The more detailed structure of the SRM can be seen in Fig. 6. The surface of the Earth and Sun will be divided into segments, of area  $A$ , with equal latitude and longitude spacing. At the centre of each segment there will be a node, Fig. 7, which has a surface area and central co-ordinates. The calculation of the solid angle subtended by the Earth node as seen from the Sun node is simplified by assuming that the Earth segment is a flat rather than curved but with the same area. The cross-sectional area of the sheet is then found by considering the angle of incidence of the light path in relation to this sheet, which is the angle between the light path and the surface normal,  $\phi$ . The solid angle is then found in the conventional manner (15) using the distance between the nodes,  $r$ ;

$$\Omega = \frac{A \cos \phi}{r^2} \quad (15)$$

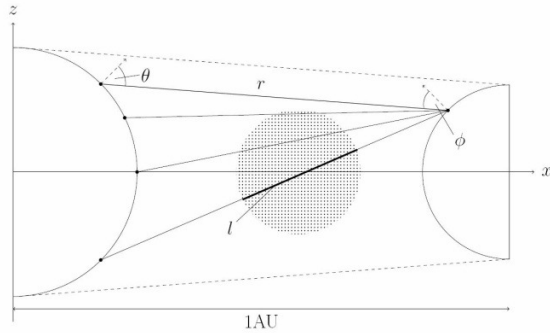


Fig. 6: Structure of the SRM where the dashed line shows the extent of the ‘useful zone’ for insolation reduction.

Clearly more accurate simulations will use a larger numbers of nodes. This is because as the surface area of each node decreases the assumption of a flat sheet becomes more accurate and also the angle  $\theta$  will better represent the whole segment. For the same reason the estimation of the path length through the cloud will be more appropriate for the surface segment.

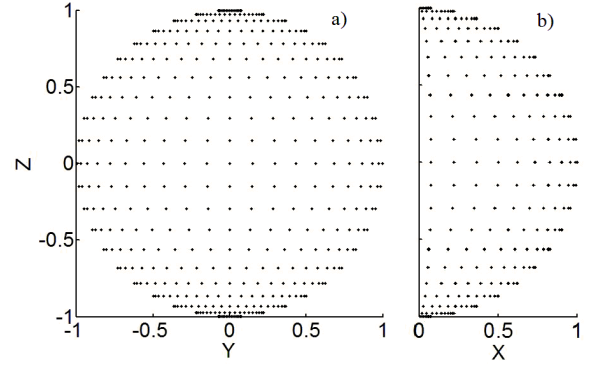


Fig. 7: Distribution of 21x21 nodes on a spherical surface, as used in the solar radiation model, viewed from the opposite body a) and perpendicular to the Sun-Earth axis b).

The path length through the cloud is calculated by the use of a numerical quadrature method in combination with a Heaviside function. For each point along the path length integral the distance to the cloud centre is found. If this point lies within the cloud radius the Heaviside function returns a value of 1 or 0 otherwise. The integral is then evaluated to determine the total path length through the cloud. This path length is then an input to the Beer-Lambert equation in (13). The solar flux transmitted from each Sun node to each Earth node is calculated, and hence the flux received by each segment of the Earth’s surface can be determined and an intensity map can be constructed.

For the case of a cloud that has been propagated using the transition matrix, the method involved in calculating the path length is slightly different. The inverse transition matrix relationship (11) can be used to find the initial position of any point along the path length integral. If the initial position is found to lie inside the sphere then the Heaviside function will return a value of 1. The density of the cloud at time  $t$  is found by dividing the initial density by the absolute value of the Jacobian determinant. This is used as it determines the volume of the phase space in relation to the initial cloud [14]. It should be noted that this paper assumes the initial velocity to be zero, hence is described by the Dirac delta function, and the initial position is described by the Heaviside function. In contrast, [14] describes the initial position using the Dirac delta function and the initial velocity using the Gaussian distribution. Due to this the absolute value of the Jacobian determinant, (16), is;

$$\|J\| = \left\| \frac{\partial v(t)}{\partial v(t_0)} \right\| \quad (16)$$

### III.II Model Testing

To test the accuracy of the SRM, the average solar insolation over the Earth's surface can be found for different numbers of longitude and latitude nodes. The results can be seen in Fig. 8. This shows that as the number of nodes increases the solar constant levels off quickly to a value of  $1381.9 \text{ W m}^{-2}$ . This value compares favourably against those found in literature e.g.  $1367 \text{ W m}^{-2}$  [4] or  $1371 \text{ W m}^{-2}$  [11] as there is an  $\approx 1\%$  difference at the highest number of nodes used.

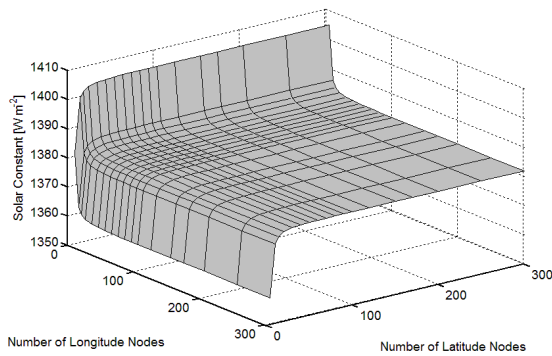


Fig. 8: Average solar constant over the Earth's surface obtained using the SRM for varying numbers of longitude and latitude nodes on the surface of the Sun.

A similar test was carried out to determine the number of longitude and latitude nodes required on both surfaces to provide a reliable result of the insolation change. This test essentially aims to determine the node number where a further increase would lead to a negligible change in the result. This was performed by placing a spherical cloud of radius  $4000 \text{ km}$  with a grain size of  $10 \mu\text{m}$  and density of  $110 \text{ m}^{-3}$  at the  $L_1$  position. The solar constant on the Earth's surface was then calculated for varying numbers of nodes on the surfaces of both bodies with the number of longitude and latitude nodes being equal. The result of this test can be seen in Fig. 9. This shows a similar shape to that seen in Fig. 8 and it can be concluded that node numbers of  $61 \times 61$  is the minimum number necessary to produce a consistent result. The motivation for finding the minimum number of nodes is to minimise the computation costs. For example, a simulation involving  $41 \times 41$  nodes on each sphere requires 15 times more path length calculations in comparison to a  $21 \times 21$  simulation.

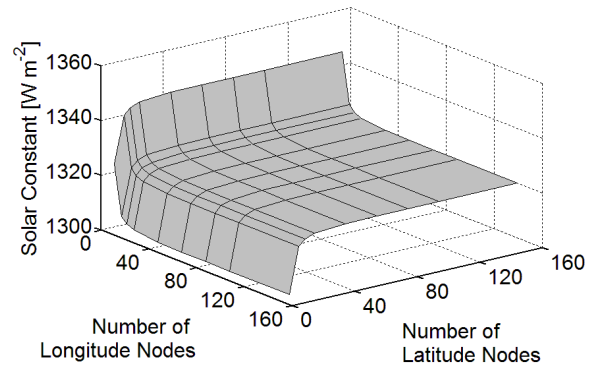


Fig. 9: Average solar constant on the Earth's surface calculated for varying node numbers in a test of the SRM using a  $4000 \text{ km}$  cloud placed the  $L_1$  point.

## IV. RESULTS

### IV.I Stability Analysis

The stability analysis begins by considering the simplest case, a spherical cloud of dust of uniform density with a grain  $\beta$ -value of zero placed at the  $L_1$  point. For all cases considered the initial velocity is assumed to be zero. For various radii of cloud the movement of a sample of evenly spaced test particles can be observed using the transition matrix (9). The lifetime of a particle is then determined to be the length of time that it is in a position to block solar photons near the Sun-Earth line. The boundary of this 'useful zone' can be seen in Fig. 6. For radii from  $500$ – $14,000 \text{ km}$  the average lifetime of these test particles can be seen in Fig. 10. The maximum size of  $14,000 \text{ km}$  was chosen as this is the approximate extent of the useful zone at the  $L_1$  point. It can clearly be seen that the average lifetime of the particles decreases significantly with cloud radius. This result sets a limit for later stability analyses as the effect of SRP is not added. It is expected, therefore, that for the scale of dust grains investigated the average lifetime of the dust particles will fall below this level when the cloud remains at the  $L_1$  point. In contrast it is expected that the average lifetime of a cloud placed at the displaced equilibrium position should increase slightly with  $\beta$  due to the reduced change of the potential function around this position.

The average lifetime of a cloud positioned at the  $L_1$  point for varying radii and  $\beta$  can also be seen in Fig. 10. This shows that when SRP is taken into account the average lifetime of the cloud decreases significantly when placed at the classical  $L_1$  point, as expected. This is irrespective of cloud radius, though the smaller clouds do show a slightly increased average lifetime. As noted previously, this is due to

the increased displacement from the classical equilibrium point. In contrast, when a cloud is centred at the new displaced equilibrium point the average lifetime increases with  $\beta$ , Fig. 11. Again the smaller cloud radii have the longer lifetimes. This increased lifetime is due to the potential function appearing flatter due to the decrease in the effect of solar gravity. Comparing these results clearly indicates that a cloud placed at the displaced equilibrium point is a more mass efficient option. However, it cannot yet be concluded that the equilibrium point is the most suitable position without taking into account the engineering challenges involved.

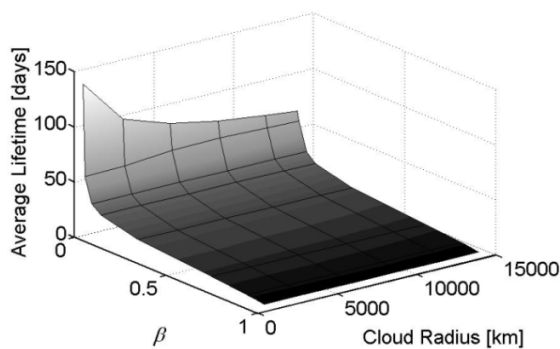


Fig. 10: Average lifetime of particles in a dust cloud positioned at the classical L<sub>1</sub> point for varying radii and values of  $\beta$ .

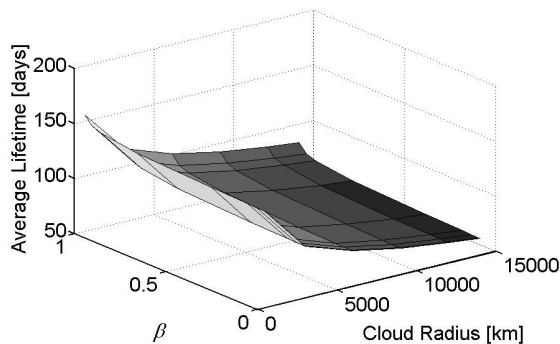


Fig. 11: Average lifetime of particles in a dust cloud positioned at the displaced equilibrium point for varying radii and values of  $\beta$ .

#### IV. II Solar Radiation Model Results

The SRM was used to determine the required mass of dust to achieve an average solar insolation of 1.7% for the case of a static cloud placed at the L<sub>1</sub> point for several scenarios. The mass was found for four different cloud radii, 1,000km, 4,000km, 8,000km and 12,000km and six different grain radii increasing by an order of magnitude from 1nm to

100 $\mu$ m. This was achieved by optimising the number density of particles within the cloud. The results of this analysis can be seen in Fig. 12 where the mass density of the grains is assumed to be 3,500 kg m<sup>-3</sup>. As can be seen, the optimum cloud radius is 4,000km for all grain radii due to the solar angle of the Sun as view from the Earth. It will be expect that for the case where the transition matrix is combined with the SRM a similar optimum radius will be found.

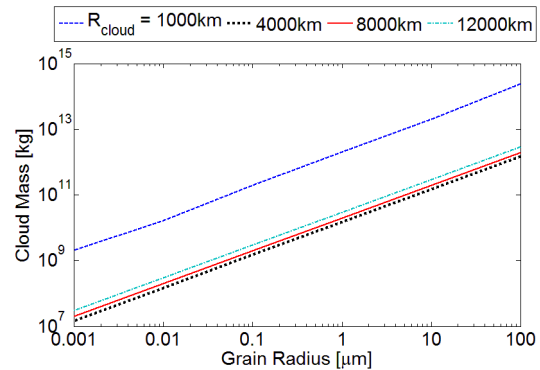


Fig. 12: The total grain mass required to achieve a 1.7% change in solar insolation for the case of a stationary cloud placed at the classical L<sub>1</sub> point.

#### IV.III Solar Radiation Model with the Transition Matrix

The key parameter for this method of geoengineering is the cloud mass necessary to create the required level of solar insolation reduction. This shall be quantified in terms of the mass per year of asteroid material required. This is calculated using the SRM by the method described in Section III.I which allows the path length through the cloud to be calculated for any given time. Hence, the evolution of the reduction in solar insolation due to the cloud dynamics can be found for different initial cloud and grain radii.

The results shall be found for dust clouds placed at the classical Lagrange point and the new displaced equilibrium points created for the different  $\beta$ -values of the asteroidal material. The initial clouds are assumed spherical with sizes ranging from 500-12000km for four different grain sizes. These grain dimensions are based on the investigation performed by Wilck and Mann [12] and are radii of 32, 10, 3.2 and 0.01 $\mu$ m which correspond to  $\beta$ -values of 0.05, 0.018, 0.061 and 0.106 respectively as seen in Fig. 3. In terms of terrestrial aerosol particles the three larger grain sizes correspond to relatively coarse particles e.g. terrestrial silt particles blown up by the wind. In contrast the 0.01 $\mu$ m particle corresponds to the size of condensed gas particles. The equilibrium points for the different particles are displaced sun-wards of the

conventional  $L_1$  point by 57,000km, 32,000km, 9,000km and 2,500km for the  $\beta$ -values used from 0.106 to 0.005 respectively. The grain size of  $0.01\mu\text{m}$  was chosen rather than a more intermediate size as it is likely to provide a more optimum solution than the grain sizes in the range  $0.01 > R_g > 3.2\mu\text{m}$ . This is because within this range the  $\beta$ -value peaks, as seen in Fig. 3, and therefore the particle lifetime is likely to be shorter. In addition, the mass of the grains within this range will also be greater than for the size of  $0.01\mu\text{m}$  chosen and hence the combination of these circumstances means the mass requirement is likely to be higher than for the other points chosen.

Each result was calculated using 20 time steps with the size of each step dependent upon the lifetime of the cloud. A steady state solution is then calculated using the combined effect of the cloud at each time step by invoking the more complex version of the Beer-Lambert law (12). Following this, the initial density of the cloud was optimised in MATLAB. Subsequently, knowing the time step and grain properties, the mass that is required to be ejected per year can be determined. The results for all four grain sizes for clouds ejected at the  $L_1$  point can be seen in Fig. 13.

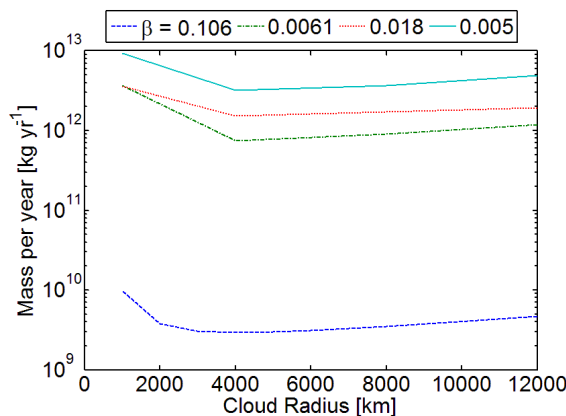


Fig. 13: Mass requirement of dust for the steady state solution of clouds ejected at the  $L_1$  point for varying initial cloud radii for the four grain sizes used.

In general the result expected was that the larger particles, which have smaller  $\beta$  values, would require less mass per year due to their greater average lifetime. This is not the case however and it appears that the decrease in grain size provides a greater mass saving than the longer lifetime of the larger particles with the optimum solution occurring for a grain radius of  $0.01\mu\text{m}$ .

For the optimum cloud radius of 3750km, which is similar to the stationary SRM result, the mass requirement is  $2.93 \times 10^9 \text{ kg yr}^{-1}$ . In comparison to the

method proposed by Struck this is a mass saving of several orders of magnitude. For this scenario the average mass ejection rate must be of order  $93 \text{ kg s}^{-1}$ . The feasibility of this estimate will be discussed later.

The results for the steady state solution for a cloud ejected at the equilibrium point can be seen in Fig. 14. It shows a similar shape to the results shown in Fig. 13 however the optimum cloud radius is shifted to 3,000km for the  $0.01\mu\text{m}$  grain radius. For this case the mass requirement is  $8.87 \times 10^8 \text{ kg yr}^{-1}$ .

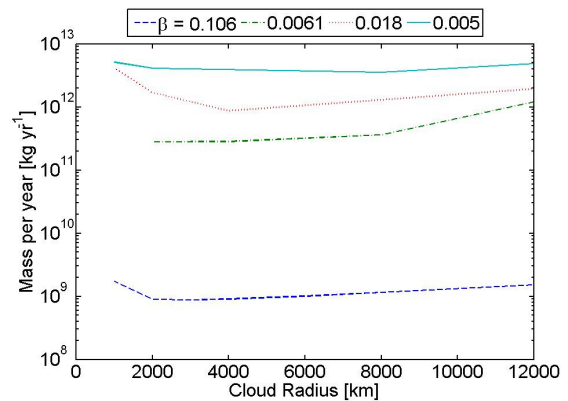


Fig. 14: Mass requirement of dust for the steady state solution of clouds ejected at the new displaced equilibrium points of the four grain radii used for varying initial cloud sizes.

The result for the case of a  $0.01\mu\text{m}$  grain is clearly better for larger grains in more than just the mass requirement. Although this is partly a product of the method used to generate the steady state solution, it still illustrates that the shorter lifetime of the smaller radius particles requires the insolation change to be achieved in a shorter time than for the larger particles. Fig. 15 shows the time to achieve a steady-state for grain radii of  $0.01\mu\text{m}$  and  $32\mu\text{m}$  where at each time step a new cloud is released. As can be seen, the  $0.01\mu\text{m}$  case reaches the desired insolation change in approximately one month whilst the  $32\mu\text{m}$  case takes of order 100 days.

The same principle applies to the deactivation period for the cloud. When geoengineering is no longer required, or if the cloud proves to have unforeseen side-effects on the Earth's climate and must be discontinued, then the lower grain size cloud will be beneficial since the cloud will disperse in a much shorter time. This will not apply to a scheme where the cloud is released at the classical equilibrium point however as the smaller particles are likely to have a longer lifetime.

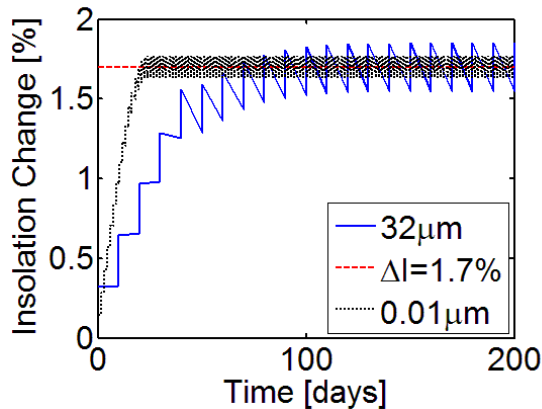


Fig. 15: Variation in insolation change expected during the activation phase of the geoengineering method for the case of a cloud of 32µm and 0.01µm sized grains placed at the L<sub>1</sub> point for a final insolation change of 1.7%.

The change in insolation seen in Fig. 15 appears highly uneven. This is due to the periodic mass ejections used to generate the steady state condition. Further research will be performed with the purpose of developing a steady state condition based on a continuous ejection of mass. In this future scenario there will be no such ‘flickering’ effect as is seen here.

The insolation change over the Earth’s surface for a cloud of radius 4000km and grain size 0.01µm released at the L<sub>1</sub> point and the new displaced equilibrium point can be seen in Fig. 16 and Fig. 17 respectively using the SRM detailed in section III. It should be noted that the tilt of the Earth’s axis is not taken into account. As can be seen, the schemes where the cloud is released at the new displaced equilibrium point show a more symmetrical pattern. The greatest insolation change naturally is located at the centre of the Earth’s disk as the cloud is positioned directly along the Sun-Earth line. This is additionally caused by the largest dispersion of the cloud occurring within the ecliptic plane whilst dispersion does not occur along the z-axis. On a basic level the occurrence of the greatest insolation change along the ‘equator’ may appear beneficial, though this may not prove to be the case as the polar regions of the Earth are the most sensitive to climate change. The insolation change map for the case of a cloud released at the classical L<sub>1</sub> point shows a different pattern. Here the insolation change is shifted towards one side of the Earth due to the movement of the cloud away from the initial position being in one direction. This will lead to greater shading in the ‘morning’ region of the Earth. The effects of this are not yet known, but an attempt to quantify this will be an interesting avenue of future research.

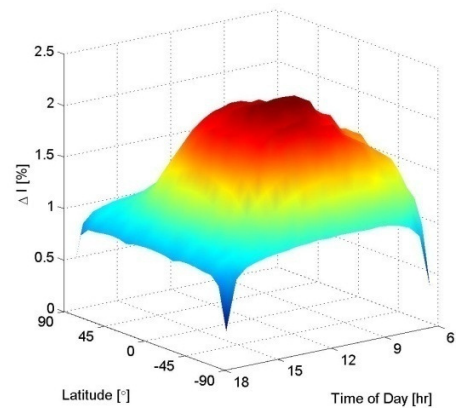


Fig. 16: Percentage insolation change over the surface of the Earth for the steady state solution of an initial cloud of radius 4000km and grain size of 0.01µm released at the classical L<sub>1</sub> point.

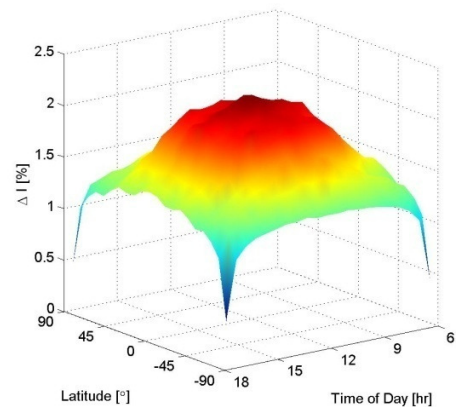


Fig. 17: Percentage insolation change over the surface of the Earth for the steady state solution of an initial cloud of radius 4000km and grain size of 0.01µm released at the displaced equilibrium point.

## V. DISCUSSION

From Section IV the mass of asteroidal material required to create an insolation change of 1.7% for dust clouds placed at the classical Lagrange point and new displaced equilibrium point has been calculated to be  $2.93 \times 10^9 \text{ kg yr}^{-1}$  and  $8.87 \times 10^8 \text{ kg yr}^{-1}$  respectively. This is considerably lower than the geoengineering methods suggested by Struck and Pearson. Finally, the engineering requirements must be discussed to determine the feasibility of this method.

### V.I. Material Availability

The mass requirements calculated are both significant, however they may not be prohibitively large. For example, work is currently being undertaken to determine the feasibility of capturing near Earth asteroids. The results of this work suggests that a relatively large amount of mass can be captured using a modest  $\Delta v$  [15]. For example capturing an asteroid such as Apophis, with an estimated mass of  $2 \times 10^{10}$  kg [16], could sustain the optimum L<sub>1</sub> and displaced equilibrium point clouds for approximately 7 and 23 years respectively. This means that relatively few asteroids are required to be captured for this method to be possible.

### V.II Cloud Generation

There are several possible methods for generating a dust cloud, these being sublimation of material from the surface, direct extraction and ejection of material from the asteroid using a mass driver and spin fragmentation. The feasibility of using these methods will now be discussed based on their ability to produce the required size of material, the required shape of cloud and their technological readiness.

#### Solar Collector/Sublimation

The sublimation method involves heating the surface of an asteroid to high temperatures such that material sublimates directly from a solid to a gas. This technique has been investigated for asteroid hazard mitigation and is a novel approach that can either be performed with a laser or a large solar collector. The latter method was first proposed by Melosh et al. [17] and will be the method discussed here.

An analysis of the physical principles and practical implications of this method was examined by Kahle [18]. It was concluded that the plume of material created is analogous to the expansion of a gas exiting a nozzle into a vacuum. The mass flux,  $Z$ , leaving the asteroid and the average velocity,  $v$ , of the particles can be estimated using the relationships in (17) and (18) respectively;

$$Z = \frac{P_{spot}}{\sqrt{2\pi R_s T_{spot}}} \quad (17)$$

$$v = \sqrt{\kappa R_s T_{spot}} M_n \left( 1 + \frac{\kappa - 1}{2} M_n^2 \right)^{-1/2} \quad (18)$$

For an S-class asteroid, comprised mostly of silicate based minerals, it is acceptable to assume that

it is comprised solely of forsterite. It follows that the specific gas constant,  $R_s$ , for diatomic forsterite has a value of  $206.7 \text{ J kg}^{-1} \text{ K}^{-1}$  and that the gas pressure at the beam spot,  $p_{spot}$ , can be calculated as follows;

$$p_{spot} = C_1 e^{C_2/T_{spot}} \quad (19)$$

Here the constants  $C_1$  and  $C_2$  have the values  $7.62 \times 10^{13} \text{ Pa}$  and  $-65,301 \text{ K}$  respectively. The spot temperature,  $T_{spot}$ , was shown by Kahle to increase with the illumination time of the spot before reaching a value in the region of  $2280 \text{ K}$ .

Kahle concluded that for a solar collector with a diameter of  $630 \text{ m}$  creating a spot of diameter  $16 \text{ m}$  the mass flux is  $16 \text{ g m}^{-2} \text{ s}^{-1}$ . This results in a mass flow rate is  $3.2 \text{ kg s}^{-1}$ . This means that for the mass ejection rate requirements of the clouds ejected at the classical L<sub>1</sub> and new displaced equilibrium points to be met, 29 and 9 solar collectors respectively would be required. This is a significant requirement, especially considering each of the spacecraft envisaged by Kahle would have a mass in the region of  $5,000 \text{ kg}$ . However, this remains considerably lower than the quantity of solar reflectors required to create the total insolation change in conventional approaches to geoengineering.

The velocity of the ejected plume can be estimated to be  $741 \text{ m s}^{-1}$  at the throat when the heat capacity ratio,  $\kappa$ , is 1.4 and the Mach number,  $M_n$ , at the throat is 1. After this the gas will expand, increasing in speed until the transition boundary between the continuum and free-molecular flows is reached. After this point the velocity is constant. By following the principles described in Kahle the velocity at this point can be found to be  $1.79 \text{ km s}^{-1}$ . This velocity is too high for the assumptions of the static cloud in this paper to hold and therefore further studies must be performed on clouds with a low initial velocity.

The ejected gas particles will be in the region  $0.2 \text{ nm}$  in diameter and as such will be considerably smaller than the scale used in this paper. Additionally the  $\beta$ -value for this scale of particle is not known. It is quite probable however that once ejected, the gas particles will re-condense to form larger particles though the scale of this effect cannot be determined. Furthermore it can be assumed that some particles will be emitted from the spot which are larger than the suggested size as some grains will be ejected by the flow of gas before being completely sublimated. Such particles will likely have lower velocities than the gas plume due to the equipartition theorem. These considerations may improve the feasibility of this method.

### Mass Driver

A mass driver concept would involve a spacecraft landing on the surface of a suitably large asteroid and then extracting material from the surface. This material would then be ejected using the mass driver. The extraction technique would be required to generate the correct, or similar, length scale of dust material and therefore some processing will likely be required.

Mass drivers are generally envisaged as high velocity devices, most suitable for launching objects into orbit cheaply and efficiently. However, they could also be used for low ejection velocity applications. An advantage of this method is that the ejection velocity can be more greatly controlled than for the solar collector method.

The use of mass drivers for asteroid hazard mitigation has previously been investigated for a spacecraft design that incorporates a solar powered mass driver [19]. A swarm of these 500-1000kg spacecraft are envisaged landing on an asteroid and ejecting material from the surface with a velocity of 100 m s<sup>-1</sup> at the rate of approximately 100 kg hr<sup>-1</sup>. As with the case of the solar collector spacecraft, several of these units would be required to meet the ejection rate demands, in the region of several thousand. However these vehicles have been designed to maximise the impulse generated on the host asteroid and hence may not be best suited for the scenario envisaged in this paper. Additionally, as with the case of the solar collector the velocity of the ejecta may not be optimum for this scenario and therefore it can be imagined that, assuming the same spacecraft power consumption, a significantly greater mass of material could be launched at lower velocities.

### Spin Fragmentation

An additional method of cloud generation is the possibility of imparting angular momentum to an asteroid such that the rotation rate increases. It is considered that a large number of small asteroids are ‘rubble piles’ [20] loosely held together by self-gravity, and as such material could easily be ejected from the surface under the correct conditions.

The angular velocity required,  $\omega_{crit}$ , to cause the liberation of material can be estimated by equating the centripetal and gravitational forces. This relationship, (20), can be found to depend only on the mass,  $M_a$ , and radius,  $R_a$ , of the asteroid and is;

$$\omega_{crit} = \sqrt{\frac{GM_a}{R_a^3}} \quad (20)$$

It has been suggested that a sub-kilometre sized asteroid can be spun-up to the point of fragmentation

by the use of tethered satellites transferring torque to it in the same manner as a reaction wheel [21]. The scale of material ejected in this scenario is likely to vary greatly as it will depend on the grain size of the surface of the asteroid. It is unlikely that the material could be ejected at the displaced equilibrium point and hence this method of cloud generation is best suited for creating clouds at the L<sub>1</sub> point. An additional factor that must be considered is that the cloud shape obtained from spinning an asteroid is likely to be a disk rather than a sphere. Further research into the stability and attenuation properties of a disk shaped cloud must be researched to fully determine the feasibility of this cloud generation method.

### V.III Comparison to solar reflector manufacture in-situ

An interesting comparison for the proposed geoengineering scheme is with manufacturing solar reflectors in-situ using captured asteroid material. At a qualitative level this may be a viable scheme, given the appropriate technology becomes available, and it may have some significant advantages over terrestrial based manufacture and launch. As well as the key advantage that the reflectors will not need to be launched to L<sub>1</sub>, the conditions for manufacturing may be superior in space. As suggested by Lippman [22] the main limitations on the thinness of manufacturing films are gravity, electrostatics and contamination. An additional factor is the oxidation of the film which will change the reflective properties of the surface and hence the perturbation by SRP. As such solar reflectors manufactured in the vacuum of space are likely to be of higher quality than terrestrial manufacture. The disadvantage in this method however is that the manufacture process will most likely need to be automated which will increase the level of complexity greatly. Lippman used the example of a heliogyro film to analyse the feasibility of such manufacturing techniques in laboratory experiments. A deposition rate of 0.2 kg hr<sup>-1</sup>, corresponding to an area 27.8 m<sup>2</sup> hr<sup>-1</sup>, was found to be achievable though no comment was made on higher deposition rates.

There is some further precedent to automated manufacture, for example recently commercialised 3D printers. Given future technological development it may be possible to ‘print’ solar reflectors in-situ given the correct bulk material is available. This again leads to the possibility of capturing asteroids from which material can be extracted and used in manufacture. For example an M class asteroid is mostly comprised of iron and nickel elements which could be used in the fabrication of reflectors. Additionally, S-class asteroids are mostly comprised

on silicate based minerals such as forsterite which also contain large amounts of magnesium which would also be a suitable material for reflector manufacture.

A model can be constructed to estimate the time scale required to manufacture the required area of solar reflectors, suggested by McInnes to be of order  $6.57 \times 10^6 \text{ km}^2$  [7] given several different scenarios. The first scenario will estimate the time taken to eject the required mass of material from an asteroid, using the plume model suggested by Kahle [18], given an initial solar collector diameter of 630m, while assuming there is no time lag required to manufacture the reflectors. The second scenario will estimate the time required for manufacture by selecting the longest time from either the time to gather the material or the time to deposit based on different deposition rates. The results can be seen in Fig. 18.

This clearly shows that the manufacturing rate is the major limiting factor with the highest value of  $1 \times 10^6 \text{ kg hr}^{-1}$  requiring in the region of 30 years to produce the necessary area of solar reflector. Should the technology become feasible, there are advantages to this approach as the time required for manufacture enables observations of changes in the Earth's climate to be made before fully committing to the scheme.

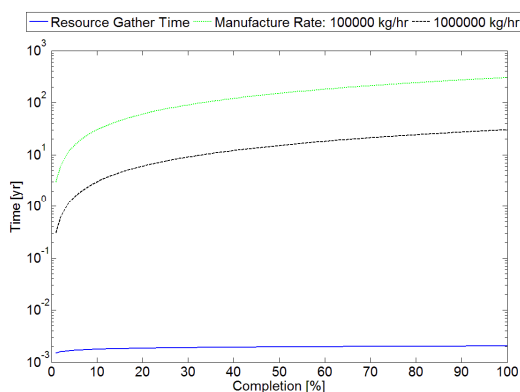


Fig. 18: Manufacturing times for the required area of thin film solar reflectors suggested by McInnes [7] for different mass deposition rates for in-situ fabrication.

#### V.IV Asteroid Stabilisation

A key technological requirement is the ability to stabilise an asteroid at or near L<sub>1</sub>. It is likely to be possible for this to be achieved using the mass ejection methods discussed previously e.g. the solar collector or the mass driver. As already stated these methods are most commonly investigated with the aim of providing an impulse to an asteroid for hazard mitigation purposes and hence this is not unfeasible.

The requirement to have multiple mass ejectors to achieve the mass ejection rate requirements will prove to be an advantage in terms of the control available over the asteroid. Using multiple thrust vectors will enable a more precise stabilisation to be achieved. It should be noted that thin film reflectors deployed near L<sub>1</sub> will also required active stabilisation of a system with a significant mass.

## VI. CONCLUSION

In this paper a method of geoengineering has been proposed involving clouds of dust placed in the vicinity of the L<sub>1</sub> point as an alternative to the use of thin film reflectors. It has been concluded that the mass requirement for a cloud placed at the classical L<sub>1</sub> point, to create an average solar insolation reduction of 1.7% is  $2.93 \times 10^9 \text{ kg yr}^{-1}$  whilst a cloud placed at a displaced equilibrium point created by the effect of solar radiation pressure is  $8.87 \times 10^8 \text{ kg yr}^{-1}$ . These mass ejection rates are considerably less than the mass required in the method proposed by Struck [6] and, for a cloud ejection period of 10 years, they are comparable to the thin film reflector methods proposed by Angel [10], McInnes [7] and others. It is envisaged that the required mass of dust can be extracted from captured near Earth objects [15], stabilised in the required position using the impulse provided by solar collectors or mass drivers used to eject material from the surface.

## ACKNOWLEDGMENTS

The work report in this paper was funded by the European Research Council through VISIONSPACE (project 227571).

## REFERENCES

1. IPCC, *Contribution of Working Groups I, II and III to the Fourth Assessment Report of the Intergovernmental Panel on Climate Change*. Core Writing Team, Pachauri, R.K. and Reisinger, A. (Eds.), IPCC, Geneva, Switzerland. pp 104, 2007.
2. Shepherd, J., et al., *Geoengineering the climate*. Report of Royal Society working group of geo-engineering, 2009.
3. Govindasamy, B. and K. Caldeira, *Geoengineering Earth's radiation balance to mitigate CO<sub>2</sub>-induced climate change*. Geophysical Research Letters, 2000. **27**(14): p. 2141-2144.

4. Govindasamy, B., K. Caldeira, and P.B. Duffy, *Geoengineering Earth's radiation balance to mitigate climate change from a quadrupling of CO<sub>2</sub>*. Global and Planetary Change, 2003. **37**(1-2): p. 157-168.
5. Pearson, J., J. Oldson, and E. Levin, *Earth rings for planetary environment control*. Acta Astronautica, 2006. **58**(1): p. 44-57.
6. Struck, C., *The feasibility of shading the greenhouse with dust clouds at the stable lunar Lagrange points*. Journal of the British Interplanetary Society, 2007. **60**(3): p. 82-89.
7. McInnes, C.R., *Space-based geoengineering: challenges and requirements*. Proceedings of the Institution of Mechanical Engineers, Part C: Journal of Mechanical Engineering Science, 2010. **224**(3): p. 571-580.
8. Early, J.T., *Space-based Solar Shield to Offset Greenhouse Effect*. JBIS, 1989. **42**(12): p. 567-569.
9. Mautner, M., *A Space-based Solar Screen against Climatic Warming*. JBIS, 1991. **44**(3): p. 135-138.
10. Angel, R., *Feasibility of cooling the Earth with a cloud of small spacecraft near the inner Lagrange point (L1)*. Proceedings of the National Academy of Sciences, 2006. **103**(46): p. 17184-17189.
11. de Pater, I. and J.J. Lissauer, *Planetary Sciences*. 2001: Cambridge University Press.
12. Wilck, M. and I. Mann, *Radiation pressure forces on "typical" interplanetary dust grains*. Planetary and Space Science, 1996. **44**(5): p. 493-499.
13. Koon, W.S., et al., *Dynamical Systems, the Three-Body Problem and Space Mission Design*. 2006: Marsden Books.
14. Sanchez, J.-P., *Asteroid Hazard Mitigation: Deflection Models and Mission Analysis*, in *Department of Aerospace Engineering*. 2009, University of Glasgow.
15. Sanchez, J.P. and C. McInnes, *Accessibility of the resources of near Earth space using multi-impulse transfers*, in *Astrodynamics Specialist Conference*. 2010, AIAA: Toronto, Ontario, Canada.
16. Binzel, R.P., et al., *Spectral properties and composition of potentially hazardous Asteroid (99942) Apophis*. Icarus, 2009. **200**(2): p. 480-485.
17. Melosh, H.J.e.a., *Non-Nuclear Strategies for Deflecting Comets and Asteroids*, in *Hazards Due to Comets and Asteroids*, T. Gehrels, Editor. 1994, University of Arizona Press.
18. Kahle, R., et al., *Physical limits of solar collectors in deflecting Earth-threatening asteroids*. Aerospace Science and Technology, 2006. **10**(3): p. 256-263.
19. Olds, J., et al., *The League of Extraordinary Machines: A Rapid and Scalable Approach to Planetary Defense Against Asteroid Impactors*. 2004, NASA Institute for Advanced Concepts.
20. Harris, A.W., *The Rotation Rates of Very Small Asteroids: Evidence for 'Rubble Pile' Structure*. Lunar and Planetary Science, 1996. **27**.
21. Bombardelli, C., *Artificial spin-up and fragmentation of sub-kilometre asteroids*. Acta Astronautica. **65**(7-8): p. 1162-1167.
22. Lippmann, M.E., *In-space fabrication of thin-film structures*. 1972, NASA.